Journal of Computational and Applied Mathematics xx (xxxx) xxx–xxx

Contents lists available at ScienceDirect

Journal of Computational and Applied Mathematics

journal homepage: www.elsevier.com/locate/cam

Study on the efficiency in the numerical integration of size-structured population models: Error and computational cost

Q1 O. Angulo [a,*], J.C. López-Marcos [b], M.A. López-Marcos [b]

[a] Departamento de Matemática Aplicada, ETSIT, Universidad de Valladolid, Pso. Belén 5, 47011 Valladolid, Spain

[b] Departamento de Matemática Aplicada, Facultad de Ciencias, Universidad de Valladolid, Pso. Belén 7, 47011 Valladolid, Spain

ARTICLE INFO

Article history:
Received 15 October 2014
Received in revised form 23 February 2015

MSC:
92D25
92D40
65M25
65M12
35B40

Keywords:
Structured population models
Numerical methods
Efficiency

ABSTRACT

We describe a procedure which is useful to select an appropriate numerical method in a size-structured population model. We consider four different numerical methods based on finite difference schemes or characteristics curves integration. We compute an analytical approximation in terms of the discretization parameters for the theoretical error principal terms and the computational cost. Thus, we show the efficiency curve that allows to select the best relationship between the discretization parameters for each numerical method. Finally, we obtain the most efficient numerical method for each test.

1. Introduction

We will consider a well-known model describing the evolution of a population which is structured by means of a physiological variable that usually is named as size. In particular we consider a model that consists of a nonlinear partial differential equation with nonlocal terms (the population balance law)

$$u_t + (g(x, I_g(t), t)\, u)_x = -\mu(x, I_\mu(t), t)\, u, \quad x_{\min} < x < x_{\max},\ t > 0, \tag{1.1}$$

a nonlinear and nonlocal boundary condition that represents the birth law

$$g(x_{\min}, I_g(t), t)\, u(x_{\min}, t) = \int_{x_{\min}}^{x_{\max}} \alpha(x, I_\alpha(t), t)\, u(x, t)\, dx, \quad t > 0, \tag{1.2}$$

and an initial condition

$$u(x, 0) = u_0(x), \quad x_{\min} \le x \le x_{\max}, \tag{1.3}$$

* Corresponding author. Tel.: +34 983 423000x5835; fax: +34 983 423661.
E-mail addresses: oscar@mat.uva.es (O. Angulo), lopezmar@mac.uva.es (J.C. López-Marcos), malm@mac.uva.es (M.A. López-Marcos).

http://dx.doi.org/10.1016/j.cam.2015.03.022
0377-0427/

Please cite this article in press as: O. Angulo, et al., Study on the efficiency in the numerical integration of size-structured population models: Error and computational cost, Journal of Computational and Applied Mathematics (2015), http://dx.doi.org/10.1016/j.cam.2015.03.022

where $I_\mu(t)$, $I_\alpha(t)$ and $I_g(t)$ are defined by

$$I_\mu(t) = \int_{x_{\min}}^{x_{\max}} \gamma_\mu(x)\, u(x,t)\, dx, \quad t \geq 0, \tag{1.4}$$

$$I_\alpha(t) = \int_{x_{\min}}^{x_{\max}} \gamma_\alpha(x)\, u(x,t)\, dx, \quad t \geq 0, \tag{1.5}$$

$$I_g(t) = \int_{x_{\min}}^{x_{\max}} \gamma_g(x)\, u(x,t)\, dx, \quad t \geq 0. \tag{1.6}$$

The independent variables x and t represent size and time, respectively. The values $x_{\min}$ and $x_{\max}$ represent the minimum and maximum size, respectively. The dependent variable $u(x,t)$ is the size-specific density of individuals with size x at time t. We assume that the size of any individual varies according to the next ordinary differential equation

$$\frac{dx}{dt} = g(x, I_g(t), t). \tag{1.7}$$

The functions g, α and μ represent the growth, the fertility and mortality rate, respectively. These are usually called the vital functions and define the life history of an individual. Functions g, α and μ are nonnegative. Note that all the vital functions depend on the size x (the structuring internal variable) and on the time t. The explicit time dependence can reflect the influence of some environmental changes on the vital functions or a seasonal behavior of the population. These functions also depend on the total amount of individuals in the population by means of the weighted functions $I_g(t)$, $I_\alpha(t)$ and $I_\mu(t)$, which represent a way of weighting the size distribution density in order to model the diverse influence of the individuals of different sizes on the life conditions.

We can find an extensive study on physiologically structured population models, with analytical studies of aspects such as derivation, existence and uniqueness, smoothness and the asymptotic behavior of solutions in [1–3]. In particular, this size-structured population model has been studied for the last three decades and the properties of existence and uniqueness of solutions was given in [4,5]. It has been successfully applied to the study of different real population problems. In order not to be exhaustive we can mention its application to the cellular dynamics [6,7], the forest dynamics that employs a hierarchical version [8,9], *Daphnia magna* population studies [10], etc.

The increase in the biological realism in such a model is achieved at the expense of a loss in mathematical tractability. Moreover, when such models include nonlinearities and environmental dependence on the different physiological rates, the use of efficient methods that provide a numerical approach is the most suitable mathematical tool for studying the problem and, indeed, it is often the only one available. Nevertheless, the numerical approach to these equations has important drawbacks because they are usually nonlinear equations and the nonlinearities in the partial differential equation and the nonlocal boundary condition are caused by nonlocal terms. A revision of the numerical schemes proposed for the solution of this problem was made in [11]. Also, the numerical integration allows us the study of some other qualitative properties as, for example, the long-time behavior in real data problems, and they shown their effectiveness [6–8].

The choice of a suitable numerical method for the integration of the problem is an important challenge. The convergence is the main property we look for. In general, it means that the numerical solution is close to a representation of the exact solution as the discretization parameters go to zero. The order of convergence quantifies the rate of convergence of this approach with respect to the discretization parameters, and it is quite important too. Also it is necessary to evaluate the computational cost which quantifies the effort needed to obtain the numerical approximation. One way to measure it is the time spent to derive the numerical results. This time increases with the accuracy or the complexity of the numerical scheme.

In this work, we will pay attention to the relationship between the global error and the computational cost. First, we shall try to obtain the most efficient relation to solve the problem between the discretization parameters for a given numerical method. Next, we shall compare diverse numerical methods for a given problem to look for the most efficient.

The order of a numerical method depends strongly on the smoothness properties of the theoretical solution and, for example, compatibility between initial and boundary conditions must be held and the data functions should be regular. We believe that for real problems with empirical data, the conditions needed to obtain a convergence order greater than two are too demanding. On the other hand, first convergence order method presents a lack of efficiency in comparison to the second order ones. So, second order schemes maintain a good compromise between the required smoothness and the efficiency of the schemes.

We will employ four second order numerical methods developed and analyzed in different works. Two of them are based on a finite-difference discretization (Lax–Wendroff and Box schemes) [12] and the others are based on a characteristics curves integration, the first one considers all the nodes in the spatial grid, aggregation grid node method (AGN), and the second one uses a selection procedure to keep constant the number of spatial grid nodes, selection grid nodes method (SGN) [11]. We obtained their convergence order in [12,13].

In the following section, we introduce the procedure and we apply it to several theoretical test problems. In the final section, we present the procedure in a real data problem for which we do not know the exact solution. We describe briefly the employed numerical methods in the Appendix.

Please cite this article in press as: O. Angulo, et al., Study on the efficiency in the numerical integration of size-structured population models: Error and computational cost, Journal of Computational and Applied Mathematics (2015), http://dx.doi.org/10.1016/j.cam.2015.03.022

2. Analytical approximation to efficiency

The numerical methods considered involve two discretization parameters: one step size k used for the time integration, and the other one h related to the size variable. In the theoretical analysis of the error of a second order method, it is typical to obtain a bound of the global error in the form

$$\mathcal{E}_{h,k} = C_1 h^2 + C_2 k^2, \tag{2.1}$$

with C_1 and C_2 positive constants. As the parameters go to zero, we consider this expression as the representative part of the exact error and, for our purposes, we admit it as a valid approximation to the global error of a specific second order numerical method.

On the other hand, it is natural to consider that computational cost depends on the size of the problem, which is given by the size of the system of equations that can be represented in terms of the discretization parameters. In [14], it is declared that the measure of the work in complex algorithms is not linear and follows a power law. However, taking into account that we discretize two different variables in a different way, we do not use the same power for both discretization parameters (as we will see, numerical experiments corroborate such assumption). Then, we establish

$$\mathcal{C}_{h,k} = C_3\, h^a\, k^b, \tag{2.2}$$

with a and b negative real numbers, and C_3 positive. Constants C_1, C_2, C_3, a and b, that appears in the error and cost expressions of the numerical method depend on the specific problem being approximated.

From numerical simulations of the method, it is usual to analyze its efficiency through log–log efficiency charts: the vertical axis correspond to the error and the horizontal axis is the cost. So, for different values of the discretization parameters, we plot the error produced for the corresponding approximation versus the computational effort required. When we compare two different methods in the efficiency plot, we prefer the method that gives more accuracy for the same computational effort (or, in other words, the method that provides the cheapest way of obtaining a prescribed precision).

On the other hand, when we consider a specific numerical method for the approximation of a problem, we consider what the best choice of the discretization parameters is. Here, we look for the best relationship between h and k for each problem: that is, we assume that

$$k = r\, h, \tag{2.3}$$

with r a fixed positive constant. So, our purpose is to select the most efficient value of r. From expressions (2.1) and (2.2), and assuming (2.3), we can write the error in terms of the cost:

$$\mathcal{E}_h = (C_1 + C_2 r^2) \left(\frac{\mathcal{C}_h}{C_3 r^b} \right)^{\frac{2}{a+b}}. \tag{2.4}$$

In the log–log representation, we have

$$\log \mathcal{E}_h = \log \frac{C_1 + C_2 r^2}{(C_3 r^b)^{\frac{2}{a+b}}} + \frac{2}{a+b} \log \mathcal{C}_h. \tag{2.5}$$

Note that, for each r fixed, different values of h provide a line with the negative slope $2/(a+b)$ (the error decreases as the cost increases), and this slope is r independent (the lines associated to a specific method, and corresponding to different values of r, are parallel). So, the most efficient line corresponds to the value of r which minimizes the first term on the right hand size of (2.5). It is easy to see that such minimum is reached at

$$r = \sqrt{\frac{C_1}{C_2} \frac{b}{a}}. \tag{2.6}$$

So, if we compare different methods for a problem, for each method we take the optimal value of r provided by (2.6). In this comparison, one can hope that for a sufficiently small value of h, the best method comes from the line with the biggest absolute value of the slope. That is, when its computational effort satisfies that $|a| + |b|$ is minimum. However, numerical simulations for very small values of h would be unsuitable due to the effect of the rounding errors.

Now, we use a test problem to illustrate the above analysis. It satisfies the regularity hypotheses that the numerical schemes need to obtain their optimal order [13]. We consider (1.1)–(1.6) on the size interval $[0, 1]$, with the following data functions: the size-specific growth, fertility and mortality moduli

$$g(x, z, t) = 0.1\,(1 - x^4)\, \frac{z}{1 + z^2}\, (1 + \exp(-0.2\, \sin^2 t))\, \exp(0.1\, \sin^2 t),$$

$$\alpha(x, z, t) = 3\, x^2 (1 - x^2) \frac{z}{(z+1)^2} \frac{(1 + \exp(-0.1\, \sin^2 t))^2}{\exp(-0.1\, \sin^2 t)},$$

$$\mu(x, z, t) = 0.2\, z \frac{1 + x^2 + 2x^3 + \frac{\sin 2t}{2}}{\exp(-0.1\, \sin^2 t)}.$$

Please cite this article in press as: O. Angulo, et al., Study on the efficiency in the numerical integration of size-structured population models: Error and computational cost, Journal of Computational and Applied Mathematics (2015), http://dx.doi.org/10.1016/j.cam.2015.03.022

Table 1
Test problem. Errors, CPU time (seconds) and order of the Lax–Wendroff method.

$k\backslash h$	1.563E−2	7.813E−3	3.906E−3	1.953E−3
1.563E−2	1.70887E−04	4.32113E−05	1.19400E−05	4.55518E−06
	2.16	4.23	8.29	16.08
7.813E−3	1.70403E−04	4.27032E−05	1.07997E−05	2.98008E−06
	4.27	8.31 2.00	16.06 2.00	30.30 2.00
3.906E−3	1.70293E−04	4.25816E−05	1.06751E−05	2.69960E−06
	8.38	16.09 2.00	30.24 2.00	60.58 2.00
1.953E−3	1.70270E−04	4.25526E−05	1.06447E−05	2.66877E−06
	16.22	30.31 2.00	60.46 2.00	121.16 2.00

Table 2
Test problem. Errors, CPU time (seconds) and order of the Box method.

$k\backslash h$	1.563E−2	7.813E−3	3.906E−3	1.953E−3
1.563E−2	1.60938E−04	3.90024E−05	1.05184E−05	4.31543E−06
	5.98	11.63	21.23	39.31
7.813E−3	1.62287E−04	4.02536E−05	9.75213E−06	2.62964E−06
	11.66	22.52 2.00	40.45 2.00	78.79 2.00
3.906E−3	1.62628E−04	4.05910E−05	1.00647E−05	2.43809E−06
	22.54	42.56 2.00	78.18 2.00	156.29 2.00
1.953E−3	1.62713E−04	4.06757E−05	1.01491E−05	2.51628E−06
	42.95	76.83 2.00	154.93 2.00	309.97 2.00

Table 3
Test problem. Errors, CPU time (seconds) and order of the AGN method.

$k\backslash h$	1.563E−2	7.813E−3	3.906E−3	1.953E−3
1.563E−2	1.97544E−04	5.36689E−05	2.04184E−05	1.23818E−05
	8.09	9.42	12.04	17.27
7.813E−3	1.98990E−04	4.93843E−05	1.34139E−05	5.10102E−06
	27.79	30.26 2.00	35.16 2.00	44.94 2.00
3.906E−3	1.99622E−04	4.97482E−05	1.23457E−05	3.35301E−06
	105.73	110.63 2.00	120.44 2.00	140.07 2.00
1.953E−3	1.99792E−04	4.99071E−05	1.24371E−05	3.08636E−06
	413.41	423.27 2.00	442.98 2.00	482.24 2.00

The weight functions, $\phi = g$, μ and α, are taken as

$$\gamma_\phi(x) = \begin{cases} c, & 0 \le x \le 1/3 \\ c\,(2-3x)^3(54x^2-27x+4), & 1/3 < x \le 2/3 \\ 0, & 2/3 < x \le 1 \end{cases},$$

$$c = \frac{1}{21250\,\ln(5/3) - 21248\,\ln(4/3) - 71131/15},$$

and we consider as the initial size-specific density the function

$$u_0(x) = \frac{1-x}{1+x}.$$

The problem (1.1)–(1.6) has the periodic solution $u(x, t)$ given by

$$u(x,t) = \frac{1-x}{1+x}\exp(-0.1\,\sin^2 t).$$

The numerical integration for this numerical experiment was carried out on the time interval [0, 10].

The first step is to obtain, for each numerical scheme, a table with errors and cpu-times (as a measure of the computational cost). At each entry in columns two to five of Tables 1–4, for the Lax–Wendroff, Box, AGN and SGN methods respectively, the upper value represents the global error $\mathcal{E}_{h,k}$ in the maximum norm. The lower number on the left is the cpu-time measured in seconds and the lower number on the right is the order s of the method computed as

$$s = \frac{\log(\mathcal{E}_{2h,2k}/\mathcal{E}_{h,k})}{\log(2)}.$$

Each column and each row of the tables correspond with different values of the spatial and time discretization parameter, respectively. The results in the tables clearly confirm the expected second order of convergence for all of them.

Please cite this article in press as: O. Angulo, et al., Study on the efficiency in the numerical integration of size-structured population models: Error and computational cost, Journal of Computational and Applied Mathematics (2015), http://dx.doi.org/10.1016/j.cam.2015.03.022

Table 4
Test problem. Errors, CPU time (seconds) and order of the SGN method.

$k\backslash h$	1.563E−2	7.813E−3	3.906E−3	1.953E−3
1.563E−2	2.06511E−04 2.80	5.24792E−05 5.51	1.66820E−05 10.94	1.09822E−05 21.63
7.813E−3	2.17214E−04 5.21	5.25011E−05 10.27 1.98	1.29471E−05 20.40 2.02	4.15956E−06 40.66 2.00
3.906E−3	2.17952E−04 10.41	5.35886E−05 20.54 2.02	1.26666E−05 40.78 2.05	3.24574E−06 81.29 2.00
1.953E−3	2.19986E−04 20.82	5.45466E−05 41.06 2.00	1.33365E−05 81.56 2.01	3.16631E−06 162.53 2.00

Table 5
Test problem. Analytical approximations of global error and computational cost, and optimal r.

	Error	Computational cost	r_{opt}
Lax–Wendroff	$1.9\,h^2 + 6.0\text{E}-03\,k^2$	$7.3\text{E}-04\,h^{-0.93}\,k^{-0.99}$	18.32
Box	$6.1\text{E}-01\,h^2 + 8.0\text{E}-03\,k^2$	$3.6\text{E}-03\,h^{-0.86}\,k^{-0.94}$	9.18
AGN	$8.0\text{E}-01\,h^2 + 3.3\text{E}-02\,k^2$	$3.8\text{E}-03\,h^{-0.27}\,k^{-1.66}$	12.17
SGN	$8.4\text{E}-01\,h^2 + 2.6\text{E}-02\,k^2$	$1.4\text{E}-03\,h^{-0.91}\,k^{-0.94}$	5.80

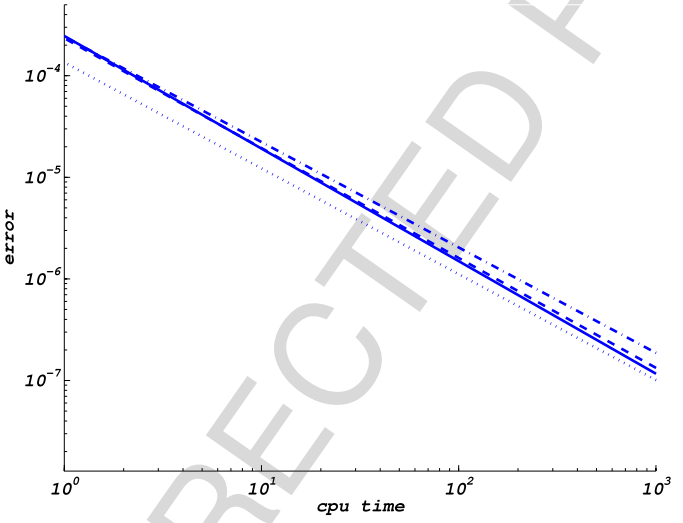

Fig. 1. Test problem. Efficiency plot. Box method solid line, Lax–Wendroff method dotted line, AGN dotted-dashed line, SGN dashed line.

The second step is to derive the values of C_1, C_2, C_3, a and b in the error and cost expressions (2.1) and (2.2). For this issue, we have used a multiple regression technique. We compute such constants with the Matlab© routine `regress`. Also, it provides R^2 (coefficient of determination which represents a quantitative measure of how well the fitted model predicts the dependent variable: if $R^2 = 1$, then the fit of the model is perfect). In Table 5, we present the analytical approximations to the global error and the computational cost (with R^2 higher than 0.99), and the optimal value of r provided by (2.6). These approximations show us that the error caused by the size-discretization is higher than the error caused by the time-discretization. This fact could be explained by the existence of nonlinearities based on nonlocal terms. With respect to the computational cost, there is an equilibrium between the size and time discretization unless the integration with the AGN method which shows a higher dominance of the time discretization due to the accumulation of grid nodes.

In Fig. 1 we present the corresponding efficiency plot, where we display the error (in the vertical axis) and the work (in the horizontal axis) in logarithmic scale. We choose for each method the value of r that represents the most efficient behavior, unless for the Lax–Wendroff method which also must satisfy the Courant–Friedrichs–Lewy (CFL) condition [15], $\hat{r} < 9.09$. We obtain in such figure that the difference methods behave better than characteristics curves methods on the error interval shown. The most efficient method correspond with the Lax–Wendroff method although the box method slope is the best. Also it is shown that the selection procedure improves the behavior of the characteristic curves methods.

Remark 1. Numerical experiments confirm the proposed expression for the computational cost formula (2.2).

Remark 2. Again, numerical experiments corroborate expression (2.1) for the global error. However, such formula would not be valid for not so smooth functions. In that case, the powers in (2.1) must be determined, for example, by means of

Please cite this article in press as: O. Angulo, et al., Study on the efficiency in the numerical integration of size-structured population models: Error and computational cost, Journal of Computational and Applied Mathematics (2015), http://dx.doi.org/10.1016/j.cam.2015.03.022

a nonlinear least-squares fitting technique (into Matlab© is developed with `lsqcurvefit` function) which provides a similar procedure.

Remark 3. Again, we have to point out that constants in formulae (2.1) and (2.2) depend on the specific problem being approximated: functions data chosen, size of the time integration considered, etc.

3. Real data case: mosquitofish population

In this section, we deal with the evolution of a mosquitofish population described in [16]. The size interval is [9, 63] and we use the following function data: the fertility rate, $\alpha(x,t) = \alpha(x)\,T_\alpha(t)$, where $\alpha(x)$ fitted to field data and

$$T_\alpha(t) = \begin{cases} \left(\frac{t}{30}\right)^3 \left(1 - \frac{t-30}{10} + \frac{(t-30)^2}{150}\right), & \text{for } 0 \le t \le 30, \\ 1, & \text{for } 30 \le t \le 90, \\ -\left(\frac{t-120}{30}\right)^3 \left(1 + \frac{t-90}{10} + \frac{(t-90)^2}{150}\right), & \text{for } 90 \le t \le 120, \\ 0, & \text{for } 120 \le t \le 365, \end{cases}$$

the growth rate $g(x,t) = g(x)\,T_g(t)$, $g(x) = \frac{63}{80.2}\left(1 - \frac{x}{63}\right)$, $9 \le x \le 63$, and

$$T_g(t) = \begin{cases} 0.2 + 0.8\left(\frac{t}{30}\right)^3 \left(1 - \frac{t-30}{10} + \frac{(t-30)^2}{150}\right), & \text{for } 0 \le t \le 30, \\ 1, & \text{for } 30 \le t \le 90, \\ 0.2 - 0.8\left(\frac{t-120}{30}\right)^3 \left(1 + \frac{t-90}{10} + \frac{(t-90)^2}{150}\right), & \text{for } 90 \le t \le 120, \\ 0.2, & \text{for } 120 \le t \le 365, \end{cases}$$

the mortality rate $\mu(x,z,t) = \mu(x,z)\,T_\mu(t)$,

$$\mu(x,z) = \begin{cases} 0.1\,\exp\left(\frac{-2000}{z}\right), & \text{for } 9 \le x \le 31, \\ 0.1\,\exp\left(\frac{-2000}{z}\right) + \left(0.023 - 0.1\,\exp\left(\frac{-2000}{z}\right)\right) & \\ \quad (x-31)^3\,(1 - 3\,(x-32)\,(65 - 2\,x)), & \text{for } 31 < x \le 32, \\ 0.023, & \text{for } 32 < x \le 63, \end{cases}$$

with $\gamma_\mu(x) = \begin{cases} 2, & 9 \le x \le 30, \\ -2\,(x-31)^3\,(1 + 3\,(x-30)\,(2\,x-59)), & 30 < x < 31, \\ 0, & 31 \le x \le 63. \end{cases}$

$$T_\mu(t) = \begin{cases} 2 - \left(\frac{t}{30}\right)^3 \left(1 - \frac{t-30}{10} + \frac{(t-30)^2}{150}\right), & 0 \le t \le 30, \\ 1, & 30 \le t \le 90, \\ 2 + \left(\frac{t-120}{30}\right)^3 \left(1 + \frac{t-90}{10} + \frac{(t-90)^2}{150}\right), & 90 \le t \le 120, \\ 2, & 120 \le t \le 365. \end{cases}$$

The numerical integration was carried out on the time interval [0, 365] (1 year). For this real situation, a theoretical solution is unknown so, for the analysis developed in the previous section, we take, for each numerical method, the numerical approximation computed on the finest grid as a representation of the exact solution. More precisely, we have employed different values of the size and time discretization parameters and we choose the finest grid values as the solution ($k = h = 7.813\text{E}-3$). We present the results on Tables 6–9, for the Lax–Wendroff, Box, AGN and SGN methods respectively. The results in the tables clearly confirm the expected second order of convergence for such methods. We have to note that, in Table 6, we show how the Lax–Wendroff method is not able to obtain the solution of the problem when the CFL condition, $r < 1.485$, is not satisfied.

With the same procedure used in the previous section, we can describe the expressions of the principal error terms and computational cost with respect to the discretization parameters and the optimal value of r, for each method, as shown in Table 10, with R^2 higher than 0.98. The behavior of the dominant error is as in the theoretical test example unless in the case of the AGN method in which the time discretization error is dominant.

Please cite this article in press as: O. Angulo, et al., Study on the efficiency in the numerical integration of size-structured population models: Error and computational cost, Journal of Computational and Applied Mathematics (2015), http://dx.doi.org/10.1016/j.cam.2015.03.022

Table 6
Mosquitofish problem. Errors, CPU time (seconds) and order for Lax–Wendroff method.

$k\backslash h$	1.250E−1	6.250E−2		3.125E−2		1.563E−2	
1.250E−1	2.386E−04 2.16						
6.250E−2	2.428E−04 4.31	5.883E−05 8.56	2.02				
3.125E−2	2.441E−04 8.61	5.982E−05 17.13	2.02	1.410E−05 34.19	2.06		
1.563E−2	2.446E−04 17.33	6.017E−05 34.51	2.02	1.444E−05 68.77	2.05	3.094E−06 138.93	2.19

Table 7
Mosquitofish problem. Errors, CPU time (seconds) and order for the Box method.

$k\backslash h$	1.250E−1	6.250E−2		3.125E−2		1.563E−2	
1.250E−1	2.049E−04 5.47	5.432E−05 10.75		2.544E−05 21.88		2.097E−05 43.30	
6.250E−2	2.025E−04 10.44	5.088E−05 20.34	2.01	1.306E−05 40.78	2.06	6.189E−06 83.90	2.04
3.125E−2	2.022E−04 20.10	5.020E−05 39.47	2.01	1.203E−05 78.39	2.08	2.750E−06 160.86	2.25
1.563E−2	2.022E−04 38.75	5.020E−05 76.17	2.01	1.203E−05 152.76	2.06	2.750E−06 313.28	2.13

Table 8
Mosquitofish problem. Errors, CPU time (seconds) and order for the AGN method.

$k\backslash h$	1.250E−1	6.250E−2		3.125E−2		1.563E−2	
1.250E−1	2.854E−05 6.20	2.854E−05 7.90		2.854E−05 11.29		2.854E−05 18.72	
6.250E−2	7.220E−06 21.91	7.220E−06 25.62	1.98	7.220E−06 33.09	1.98	7.220E−06 48.59	1.98
3.125E−2	1.891E−06 86.54	1.891E−06 94.17	1.93	1.891E−06 109.61	1.93	1.891E−06 141.13	1.93
1.563E−2	9.283E−07 356.52	9.283E−07 372.65	1.03	9.283E−07 405.10	1.03	9.283E−07 470.83	1.03

Table 9
Mosquitofish problem. Errors, CPU time (seconds) and order for the SGN method.

$k\backslash h$	1.250E−1	6.250E−2		3.125E−2		1.563E−2	
1.250E−1	1.653E−04 1.58	5.707E−05 3.14		2.991E−05 6.35		2.819E−05 12.92	
6.250E−2	1.740E−04 3.17	3.858E−05 6.30	2.10	1.031E−05 12.56	2.47	7.220E−06 25.44	2.05
3.125E−2	1.435E−04 6.35	4.748E−05 12.64	1.87	8.595E−06 25.16	2.17	2.750E−06 50.27	1.91
1.563E−2	1.368E−04 12.71	2.984E−05 25.32	2.27	1.097E−05 50.52	2.11	1.788E−06 100.85	2.27

Table 10
Mosquitofish problem. Analytical approximations of global error and computational cost, and optimal r.

	Error	Computational cost	r_{opt}
Lax–Wendroff	$1.3E-02\,h^2 + 4.9E-04\,k^2$	$3.4E-02\,h^{-0.99}\,k^{-0.99}$	5.19
Box	$1.2E-02\,h^2 + 1.1E-03\,k^2$	$1.1E-01\,h^{-0.98}\,k^{-0.92}$	3.30
AGN	$2.8E-05\,h^2 + 2.1E-03\,k^2$	$1.3E-01\,h^{-0.37}\,k^{-1.68}$	0.25
SGN	$1.2E-02\,h^2 + 2.2E-03\,k^2$	$2.6E-02\,h^{-1.00}\,k^{-0.99}$	2.27

Then we compare all the methods in the corresponding efficiency plot, Fig. 2, in which we use the optimal r for all the methods unless the Lax–Wendroff method which is limited by the CFL condition. The results confirm that the Box method is the most efficient and that the SGN is the most efficient into the characteristics methods. These conclusions are different from the ones given in [16]. In such work, we did not use the analytical expressions of the optimal r obtained in this work.

Finally, we want to add two aspects that we pointed out in [16]. The use of the finite difference methods introduces spurious oscillations that are more difficult to avoid in the case of the Lax–Wendroff one. Thus the characteristics schemes

Please cite this article in press as: O. Angulo, et al., Study on the efficiency in the numerical integration of size-structured population models: Error and computational cost, Journal of Computational and Applied Mathematics (2015), http://dx.doi.org/10.1016/j.cam.2015.03.022

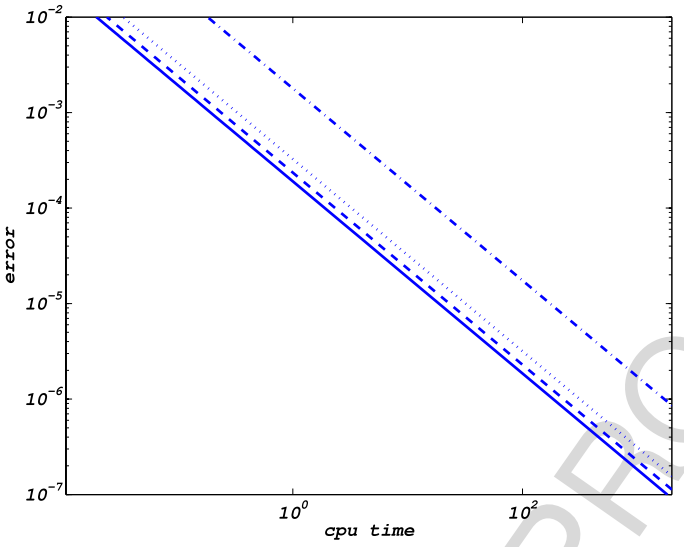

Fig. 2. Mosquitofish problem. Efficiency plot. Box method solid line, Lax–Wendroff method dotted line, AGN dotted-dashed line, SGN dashed line.

perform solutions that fit the qualitative behavior better than the finite difference methods. On the other hand, the long-time integration shows some weakness in the numerical integration with the AGN method and makes more efficient the SGN method because of the selection procedure.

4. Conclusions

We have presented a procedure to obtain an analytical approximation to the efficiency. We have used it to compare four different second-order numerical methods. We have shown the best relation between the discretization parameters for each method and we have obtained the most efficient numerical method in two situations: a theoretical example and other one based on biological data. We have limited our study to these second order techniques, however other numerical procedures would be considered.

Such comparisons depend strongly on the problem analyzed, so, we cannot expect for a numerical method which behaves better in all the possible numerical tests. Thus, for a particular problem, in which we usually have to compute numerically the solution with many different data, the most efficient method seems to be the most useful and here we establish an appropriate technique in order to compare them.

However, previous works [16] showed that not only the accuracy of the numerical approximations is an influential fact but other qualitative properties are also necessary. At least, we expect the numerical integration provides a non-negative approximation because the problem is biologically meaningful and they must keep the singularities the vital functions could present and not to introduce other misunderstandings in the solution as, for example, spurious oscillations.

In general, on a long time integration, the use of methods which preserve some of the qualitative properties of the solution can perform better. In this way, characteristics curves methods would be good candidates. Qualitative considerations should be incorporated to select a particular numerical method for a specific problem.

Acknowledgments

This work was supported in part by the project of the Ministerio de Ciencia e Innovación MTM2011-25238 and the project of the Consejería de Educación, JCyL VA191U13.

The authors are very grateful to the anonymous referees for their careful reading and their valuable aid to improve the manuscript.

Appendix. Numerical methods

A.1. The Lax–Wendroff method

Let J be a positive integer. Let the points of the grid in the size variable be $x_j = x_{\min} + j\,h$, $0 \le j \le J$, where $h = \frac{x_{\max} - x_{\min}}{J}$ is the grid diameter. We denote by k the time step, and the discrete time levels as $t_n = n\,k$, $0 \le n \le N$, $N = \left[\frac{T}{k}\right]$. The sub-index j makes reference to the grid point x_j and the super-index n to the time level t_n. Finally, we denote by U_j^n the numerical

Please cite this article in press as: O. Angulo, et al., Study on the efficiency in the numerical integration of size-structured population models: Error and computational cost, Journal of Computational and Applied Mathematics (2015), http://dx.doi.org/10.1016/j.cam.2015.03.022

approximation to $u(x_j, t_n)$, $0 \le j \le J$, $0 \le n \le N$. We suppose that an approximation to the initial condition (1.3), $\mathbf{U}^0$, is given (for example, the grid restriction of the initial data u_0).

The Lax–Wendroff method is a two-stage scheme defined for each $n = 0, 1, \ldots, N-1$. First we calculate the intermediate values in the following way

$$U_{j-\frac{1}{2}}^{n+\frac{1}{2}} = U_{j-\frac{1}{2}}^{n} - \frac{k}{2h}\left(g_j^n\, U_j^n - g_{j-1}^n\, U_{j-1}^n\right) - \frac{k}{2}\mu_{j-\frac{1}{2}}^n\, U_{j-\frac{1}{2}}^n, \tag{A.7}$$

where $g_j^n = g\left(x_j, Q_h\left(\boldsymbol{\gamma}_g\, \mathbf{U}^n\right), t_n\right), j = 0, 1, \ldots, J; x_{j-\frac{1}{2}} = \frac{1}{2}\left(x_{j-1} + x_j\right), U_{j-\frac{1}{2}}^n = \frac{1}{2}\left(U_{j-1}^n + U_j^n\right), \mu_{j-\frac{1}{2}}^n = \mu\left(x_{j-\frac{1}{2}}, Q_h\left(\boldsymbol{\gamma}_\mu\, \mathbf{U}^n\right), t_n\right), j = 1, 2, \ldots, J$. The function $Q_h(\mathbf{V}^n)$, $n = 0, 1, \ldots, N-1$, denotes the composite trapezoidal quadrature rule and products $\boldsymbol{\gamma}_s\, \mathbf{U}^n$, $s = \mu, g$, must be interpreted componentwise. In the second stage, we obtain the values U_j^{n+1}, $j = 1, 2, \ldots, J-1$, as

$$U_j^{n+1} = U_j^n - \frac{k}{h}\left(g_{j+\frac{1}{2}}^{n+\frac{1}{2}}\, U_{j+\frac{1}{2}}^{n+\frac{1}{2}} - g_{j-\frac{1}{2}}^{n+\frac{1}{2}}\, U_{j-\frac{1}{2}}^{n+\frac{1}{2}}\right) - k\,\mu_j^{n+\frac{1}{2}}\, U_j^{n+\frac{1}{2}},$$

$$U_J^{n+1} = 0,$$

where $U_j^{n+\frac{1}{2}} = \frac{1}{2}\left(U_{j+\frac{1}{2}}^{n+\frac{1}{2}} + U_{j-\frac{1}{2}}^{n+\frac{1}{2}}\right), \mu_j^{n+\frac{1}{2}} = \mu\left(x_j, Q_h\left(\boldsymbol{\gamma}_\mu\, \mathbf{U}^{n+\frac{1}{2}}\right), t_n + \frac{k}{2}\right), j = 1, 2, \ldots, J-1; g_{j+\frac{1}{2}}^{n+\frac{1}{2}} = g\left(x_{j+\frac{1}{2}}, Q_h\left(\boldsymbol{\gamma}_g\, \mathbf{U}^{n+\frac{1}{2}}\right), t_n + \frac{k}{2}\right), j = 0, 1, \ldots, J-1$. Now, $Q_h(\mathbf{V}^{n+\frac{1}{2}})$, $0 \le n \le N-1$, denotes the composite mid-point quadrature rule. Finally, the approximation U_0^{n+1} to $u(x_{\min}, t_{n+1})$, for $0 \le n \le N-1$, is calculated with the condition

$$g_0^{n+1}\, U_0^{n+1} = Q_h(\boldsymbol{\alpha}^{n+1}\, \mathbf{U}^{n+1}),$$

where $g_0^{n+1} = g\left(x_{\min}, Q_h\left(\boldsymbol{\gamma}_g\, \mathbf{U}^{n+1}\right), t_n\right)$ and $\boldsymbol{\alpha}_j^{n+1} = \alpha(x_j, Q_h\left(\boldsymbol{\gamma}_\alpha\, \mathbf{U}^{n+1}\right), t_{n+1}), j = 0, 1 \ldots, J, 0 \le n \le N-1$. Again, the products $\boldsymbol{\alpha}^{n+1}\, \mathbf{U}^{n+1}$ and $\boldsymbol{\gamma}_s\, \mathbf{U}^{n+1}$, $s = g, \alpha$, must be interpreted componentwise.

A.2. The Box method

The parameters J, N, h and k, and also the mesh grid, are defined as in Appendix A.1. Again, we start with an initial condition $\mathbf{U}^0$.

We introduce the half integer grid points $x_{j-\frac{1}{2}} = \frac{1}{2}\left(x_{j-1} + x_j\right)$, $1 \le j \le J$; the mean value operators $U_j^{n+\frac{1}{2}} := \frac{1}{2}\left(U_j^{n+1} + U_j^n\right), U_{j-\frac{1}{2}}^n = \frac{1}{2}\left(U_{j-1}^n + U_j^n\right), U_{j-\frac{1}{2}}^{n+\frac{1}{2}} = \frac{1}{2}\left(U_{j-1}^{n+\frac{1}{2}} + U_j^{n+\frac{1}{2}}\right)$ and the difference operator $D\, U_j^n = U_j^{n+1} - U_j^n$.

The box method is defined by

$$\frac{D\, U_j^n + D\, U_{j-1}^n}{2\,k} + \frac{g_j^{n+\frac{1}{2}}\, U_j^{n+\frac{1}{2}} - g_{j-1}^{n+\frac{1}{2}}\, U_{j-1}^{n+\frac{1}{2}}}{h} = -\mu_{j-\frac{1}{2}}^{n+\frac{1}{2}}\, U_{j-\frac{1}{2}}^{n+\frac{1}{2}}, \tag{A.8}$$

$$g_0^{n+1}\, U_0^{n+1} = Q_h(\boldsymbol{\alpha}^{n+1}\, \mathbf{U}^{n+1}), \tag{A.9}$$

$1 \le j \le J$, $0 \le n \le N-1$, where $Q_h(\mathbf{V}^n)$ represents the trapezoidal quadrature rule, and, for $0 \le n \le N-1$: $g_j^{n+\frac{1}{2}} = g\left(x_j, Q_h\left(\boldsymbol{\gamma}_g\, \mathbf{U}^{n+\frac{1}{2}}\right), t_n + \frac{k}{2}\right), 0 \le j \le J, g_0^{n+1} = g\left(x_{\min}, Q_h\left(\boldsymbol{\gamma}_g\, \mathbf{U}^{n+1}\right), t_{n+1}\right)$; $\mu_{j-\frac{1}{2}}^{n+\frac{1}{2}} = \mu\left(x_{j-\frac{1}{2}}, Q_h\left(\boldsymbol{\gamma}_\mu\, \mathbf{U}^{n+\frac{1}{2}}\right), t_n + \frac{k}{2}\right), 1 \le j \le J$. Notation for $\boldsymbol{\alpha}^n$ as in the Lax–Wendroff method.

A.3. Aggregation grid nodes method (AGN)

The parameters J, N, h and k are defined as in Appendix A.1.

The initial grid nodes are given by $X_j^0 = x_{\min} + j\,h$, $0 \le j \le J$. We suppose that the approximations to the theoretical solution in such nodes are known, U_j^0, $0 \le j \le J$. We also suppose that at the first time level t_1, the new grid nodes, $\mathbf{X}^1$, and the corresponding solution values, $\mathbf{U}^1$, are known. Furthermore, X_j^0 and X_{j+1}^1, $0 \le j \le J-1$, are (numerically) in the same characteristic curve. Angulo and López-Marcos obtained the initial conditions by means of the well-known second order method [13].

The numerical approximations at the time level t_{n+2}, $0 \le n \le N-2$ are obtained as follows. We suppose that the numerical approximations at the previous time levels, t_n and t_{n+1}, are known, $\mathbf{X}^n$, $\mathbf{U}^n$ and $\mathbf{X}^{n+1}$, $\mathbf{U}^{n+1}$. Where X_j^n and X_{j+1}^{n+1}, $0 \le j \le J+n-1$ belong (numerically) to the same characteristic curve. We introduce the notation $\mu^*(x, I_g(t), I_\mu(t), t) =$

$\mu(x, I_g(t), I_\mu(t), t) + g_x(x, I_g(t), t)$, $Q(\mathbf{X}, \mathbf{V}) = \sum_{j=0}^{p-1} \frac{X_{j+1}-X_j}{2}(V_j + V_{j+1})$; $(\boldsymbol{\gamma}_s)_j = \gamma_s(X_j)$, $s = \alpha, g, \mu$, $j = 0, 1, \ldots, p$. This notation will be used throughout the subsection. First, the grid values at the time level t_{n+2} are calculated by

$$X_0^{n+2} = x_{\min}, \qquad X_{J+n+2}^{n+2} = x_{\max}, \tag{A.10}$$

$$X_1^{n+2} = X_0^{n+1} + k\, g\left(X_0^{n+1} + \frac{k}{2} g\left(X_0^{n+1}, Q\left(\mathbf{X}^{n+1}, \boldsymbol{\gamma}_g \mathbf{U}^{n+1}\right), t_{n+1}\right), \frac{3\,Q(\mathbf{X}^{n+1}, \boldsymbol{\gamma}_g \mathbf{U}^{n+1}) - Q(\mathbf{X}^n, \boldsymbol{\gamma}_g \mathbf{U}^n)}{2}, t_{n+1} + \frac{k}{2}\right), \tag{A.11}$$

$$X_j^{n+2} = X_{j-2}^n + 2\,k\, g(X_{j-1}^{n+1}, Q\left(\mathbf{X}^{n+1}, \boldsymbol{\gamma}_g \mathbf{U}^{n+1}\right), t_{n+1}), \quad 2 \le j \le J+n+1, \tag{A.12}$$

and the approximations to the theoretical solution in these nodes at such time level using

$$U_1^{n+2} = U_0^{n+1} \exp\left(-k\,\mu^*\left(X_0^{n+1} + \frac{k}{2} g(X_0^{n+1}, Q\left(\mathbf{X}^{n+1}, \boldsymbol{\gamma}_g \mathbf{U}^{n+1}\right), t_{n+1}), \frac{3\,Q(\mathbf{X}^{n+1}, \boldsymbol{\gamma}_g \mathbf{U}^{n+1}) - Q(\mathbf{X}^n, \boldsymbol{\gamma}_g \mathbf{U}^n)}{2}, \frac{3\,Q(\mathbf{X}^{n+1}, \boldsymbol{\gamma}_\mu \mathbf{U}^{n+1}) - Q(\mathbf{X}^n, \boldsymbol{\gamma}_\mu \mathbf{U}^n)}{2}, t_{n+1} + \frac{k}{2}\right)\right), \tag{A.13}$$

$$U_j^{n+2} = U_{j-2}^n \exp\left(-2\,k\,\mu^*\left(X_{j-1}^{n+1}, Q\left(\mathbf{X}^{n+1}, \boldsymbol{\gamma}_g \mathbf{U}^{n+1}\right), Q\left(\mathbf{X}^{n+1}, \boldsymbol{\gamma}_\mu \mathbf{U}^{n+1}\right), t_{n+1}\right)\right), \quad 2 \le j \le J+n+1, \tag{A.14}$$

$$U_{J+n+2}^{n+2} = 0. \tag{A.15}$$

The equations at the time level t_{n+2} are completed with the approximation U_0^{n+2} to $u(x_{\min}, t_{n+2})$ by means of the discretization of the boundary condition (1.2)

$$U_0^{n+2} = \frac{Q(\mathbf{X}^{n+2}, \boldsymbol{\alpha}(\mathbf{X}^{n+2}, \mathbf{U}^{n+2})\,\mathbf{U}^{n+2})}{g(x_{\min}, Q\left(\mathbf{X}^{n+2}, \boldsymbol{\gamma}_g \mathbf{U}^{n+2}\right), t_{n+2})}, \tag{A.16}$$

where $\boldsymbol{\alpha}_j(\mathbf{X}^{n+2}, \mathbf{U}^{n+2}) = \alpha\left(X_j^{n+2}, Q(\mathbf{X}^{n+2}, \boldsymbol{\gamma}_\alpha \mathbf{U}^{n+2}), t_{n+2}\right)$, $0 \le j \le J+n+2$, $0 \le n \le N-2$.

A.4. Selection grid nodes method (SGN)

The following scheme considers a modification in the grid of the previous one so that, by using a selection of the grid nodes, the number of nodes does not increase at each time level. Thus, we try to reduce the computational cost without loss of accuracy.

The grid nodes and the numerical approximations at time t_2, $\mathbf{X}^2$, $\mathbf{U}^2$, are defined by means of (A.10)–(A.16) for $n = 0$. Next, we calculate $Q^2(\mathbf{X}^2, \boldsymbol{\gamma}_\mu^2 \mathbf{U}^2)$.

At the new time level, there is a different number of nodes because a new node that fluxes through the boundary is introduced. So, at the time level t_0, we have $(J+1)$ grid nodes, at t_1 we have $(J+2)$ and at t_2 we have $(J+3)$. Now, the first grid node X_l^2 that satisfies

$$|X_{l+1}^2 - X_{l-1}^2| = \min_{1 \le j \le J+1} |X_{j+1}^2 - X_{j-1}^2|$$

is eliminated and, also X_{l-1}^1, the grid node in the same characteristic curve at t_1, is taken out. The number of nodes at the levels involved in the implementation of our two-step scheme are kept fixed: $(J+3)$ nodes for the time level reached in the integration and $(J+2)$ and $(J+1)$ for the previous ones. However, the approximations to the nonlocal terms at such time levels are not recomputed.

Now, we suppose that the numerical approximations at time levels t_n and t_{n+1} are known, and they are denoted by $\{X_0^n, X_1^n, \ldots, X_{J-1}^n, X_J^n = x_{\max}\}$, $\{U_0^n, U_1^n, \ldots, U_{J-1}^n, U_J^n = 0\}$, $Q(\mathbf{X}^n, \boldsymbol{\gamma}_s \mathbf{U}^n)$, $s = \alpha, g, \mu$, and $\{X_0^{n+1} = x_{\min}, X_1^{n+1}, \ldots, X_J^{n+1}, X_{J+1}^{n+1} = x_{\max}\}$, $\{U_0^{n+1}, U_1^{n+1}, \ldots, U_J^{n+1}, U_{J+1}^{n+1} = 0\}$, $Q(\mathbf{X}^{n+1}, \boldsymbol{\gamma}_s \mathbf{U}^{n+1})$, $s = \alpha, g, \mu$ (note that X_j^n and X_{j+1}^{n+1}, $0 \le j \le J-1$, are, numerically, in the same characteristic curve). In addition, the grid considered at t_n has lost two nodes with respect to the moment when $\mathbf{X}^n$ was actually calculated, while the grid used at t_{n+1} has only one node less than $\mathbf{X}^{n+1}$. The numerical grid nodes at the new time level t_{n+2}, are computed by means of (A.10)–(A.12), $2 \le j \le J+1$, and the approximations to the theoretical solution in these nodes are obtained using (A.13), (A.14), $2 \le j \le J+1$, and (A.15). The equations at time level t_{n+2} are completed with the approximation U_0^{n+2} to $u(x_{\min}, t_{n+2})$ using (A.16). Now, we calculate $Q(\mathbf{X}^{n+2}, \boldsymbol{\gamma}_s \mathbf{U}^{n+2})$, $s = \alpha, g, \mu$. Note that, for the time levels t_n, $n \ge 2$, the quadrature rules always use the same number of nodes $(J+3)$. Finally, we eliminate the first grid node X_l^{n+2} that satisfies

$$|X_{l+1}^{n+2} - X_{l-1}^{n+2}| = \min_{1 \le j \le J+1} |X_{j+1}^{n+2} - X_{j-1}^{n+2}|$$

and we take out X_{l-1}^{n+1}, the grid node in the same characteristic curve at the previous time level.

References

[1] J.A.J. Metz, E.O. Diekmann (Eds.), The Dynamics of Physiologically Structured Populations, in: Springer Lecture Notes in Biomathematics, vol. 68, Springer, Heildelberg, 1986.
[2] J.M. Cushing, An Introduction to Structured Populations Dynamics, in: CMB-NSF Regional Conference Series in Applied Mathematics, SIAM, 1998.
[3] B. Perthame, Transport Equations in Biology, Birkhäuser Verlag, Basel, 2007.
[4] A. Calsina, J. Saldaña, A model of physiologically structured population dynamics with a nonlinear individual growth rate, J. Math. Biol. 33 (4) (1995) 335–364.
[5] N. Kato, A general model of size-dependent population dynamics with nonlinear growth rate, J. Math. Anal. Appl. 297 (2004) 234–256.
[6] A.S. Ackleh, M.L. Delcambre, K.L. Sutton, D. Ennis, A structured model for the spread of mycobacterium marinum: foundations for a numerical approximation scheme, Math. Biosci. Eng. 11 (2014) 679–721.
[7] A.S. Ackleh, K. Deng, K. Ito, J. Thibodeaux, A structured erythropoiesis model with nonlinear cell maturation velocity and hormone decay rate, Math. Biosci. 204 (2006) 21–48.
[8] O. Angulo, R. Bravo de la Parra, J.C. López-Marcos, M.A. Zavala, Stand dynamics and tree coexistence in an analytical structured model: the role of recruitment, J. Theoret. Biol. 333 (2013) 91–101.
[9] L. Abia, O. Angulo, J.C. López-Marcos, M.A. López-Marcos, Numerical integration of a hierarchically size-structured population model with contest competition, J. Comput. Appl. Math. 258 (2014) 116–134.
[10] O. Angulo, J.C. López-Marcos, M.A. López-Marcos, Analysis of an efficient integrator for a size-structured population model with a dynamical resource, Comput. Math. Appl. 68 (2014) 941–961.
[11] L. Abia, O. Angulo, J.C. López-Marcos, Size-structured population models and their numerical solutions, Discrete Contin. Dyn. Syst. Ser. B 4 (2004) 1203–1222.
[12] O. Angulo, J.C. López-Marcos, Numerical integration of autonomous and nonautonomous nonlinear size-structured population models, Math. Biosci. 177 (2002) 39–71.
[13] O. Angulo, J.C. López-Marcos, Numerical integration of fully nonlinear size-structured population models, Appl. Numer. Math. 50 (2004) 291–327.
[14] S.F. Goldsmith, A.S. Aiken, D.S. Wilkerson, Measuring empirical computational complexity, Proc. ESEC/FSE (2007) 395–404.
[15] K.W. Morton, D.F. Mayers, Numerical Solution of Partial Differential Equations, Cambridge University, Cambridge, 1994.
[16] O. Angulo, A. Durán, J.C. López-Marcos, Numerical study for size-structured population models: a case of *Gambussia affinis*, C. R. Biol. 328 (2005) 387–402.

Please cite this article in press as: O. Angulo, et al., Study on the efficiency in the numerical integration of size-structured population models: Error and computational cost, Journal of Computational and Applied Mathematics (2015), http://dx.doi.org/10.1016/j.cam.2015.03.022